Dynamics of the sex ratio in *Tetrahymena thermophila*

Guangying Wang,*,† Kai Chen,*,† Jing Zhang,*,† Xuefeng Ma,*,† Shanjun Deng,‡ Jie Xiong,* Xionglei He,‡,§ Yunxin Fu,**,†† and Wei Miao*

*Key Laboratory of Aquatic Biodiversity and Conservation, Institute of Hydrobiology, Chinese Academy of Sciences, Wuhan, Hubei 430072, China

†University of Chinese Academy of Sciences, Beijing 100049, China

**Laboratory for Conservation and Utilization of Bioresources, Yunnan University, Kunming 650091, China

††Department of Biostatistics and Data Science, and Human Genetics Center, School of Public Health, The University of Texas Health Science Center, Houston, Texas 77030

‡Key Laboratory of Gene Engineering of Ministry of Education, Cooperative Innovation Center for High Performance Computing, College of Ecology and Evolution, Sun Yat-sen University, Guangzhou 510275, China

§State Key Laboratory of Biocontrol, School of Life Sciences, Sun Yat-sen University, Guangzhou 510275, China

Reference numbers for genome sequencing data at SRA: SRP080979

Running title: Sex ratio dynamics in *Tetrahymena*

Key words: ciliate, multi-sex system, sex ratio, population genetics, experimental evolution

Corresponding author:

Yunxin Fu

1200 Herman Pressler Street RAS E541 Houston, TX 77030, USA

Phone: 713-500-9813

E-mail: yunxin.fu@uth.tmc.edu

Wei Miao

#7 Donghu South Rd., Wuchang District, Wuhan, Hubei 430072, China

Phone: 86-27-68780050

E-mail: miaowei@ihb.ac.cn.

Abstract

Sex is often hailed as one of the major successes in evolution, and in sexual organisms the maintenance of proper sex ratio is crucial. As a large unicellular eukaryotic lineage, ciliates exhibit tremendous variation in mating systems, especially the number of sexes and the mechanism of sex determination (SD), and yet how the populations maintain proper sex ratio is poorly understood. Here *Tetrahymena thermophila*, a ciliate with seven mating types (sexes) and probabilistic SD mechanism, is analyzed from the standpoint of population genetics. It is found based on a newly developed population genetics model that there are plenty of opportunities for both the co-existence of all seven sexes and the fixation of a single sex, pending on several factors, including the strength of natural selection. To test the validity of predictions, five experimental populations of *T. thermophila* were maintained in the laboratory so that the factors that can influence the dynamics of sex ratio could be controlled and measured. Furthermore, whole-genome sequencing was employed to examine the impact of newly arisen mutations. Overall, it is found that the experimental observations highly support theoretical predictions. It is expected that the newly established theoretical framework is applicable in principle to other multi-sex organisms to bring more insight into the understanding of the maintenance of multiple sexes in a natural population.

Key words: ciliate, multi-sex system, sex ratio, experimental evolution

Introduction

Sex is often hailed as one of the most successful evolutionary inventions across eukaryotes (Weismann 1887; Bell 1982) and is fundamental for lineage survival (Speijer *et al.* 2015). This is due to various benefits provided by sex, such as speeding up adaptation by accelerating the accumulation of beneficial mutations (Fisher 1930; Muller 1932) and allowing natural selection to proceed more effectively by increasing the genetic variance in fitness (Weismann 1887; Burt 2000). For most sexual organisms, a crucial prerequisite for the occurrence of sex is that a population must maintain appropriate proportion of different sexes, or sex ratio. The strategies to adjust offspring sex ratio have been well demonstrated in a wide range of organisms with two sexes, male and female, in the context of Fisher's equal allocation theory and its extensions (West 2009). However, how organisms with multiple (>2) sexes maintain proper sex ratio in the population is still poorly understood.

Ciliates are a large unicellular eukaryotic evolutionary lineage that show rapid diversification in many aspects of the mating systems (Phadke and Zufall 2009). First, ciliates exhibit a great variation in the number of mating types (sexes), ranging from two to several or more, e.g. 100 for *Stylonychia mytilus* (Ammermann 1982). Second, the mechanisms of sex determination (SD) differ widely, ranging from Mendelian systems to developmental nuclear differentiation, either stochastic or cytoplasmic (Orias *et al.* 2017). The well-studied ciliate, *Tetrahymena thermophila*, has seven self-incompatible sexes (I–VII) that are determined by alleles at a single locus (*mat*). Unlike the sex-specific alleles (*mat-a*, *mat-alpha*) in yeast, each *mat* allele specifies the probability with which a progeny cell will express one of the seven sexes (Arslanyolu and Doerder 2000). For example, a classic B-type *mat* allele specifies the

following probabilities for each sex: I, 0; II, 0.275; III, 0.192; IV, 0.278; V, 0.076; VI, 0.041; VII, 0.138 (Nanney 1960). This particular form of sex inheritance has been called probabilistic SD and the unique distribution of probabilities is called the allele's SD pattern (Paixao *et al.* 2011). For each allele, the SD pattern is very stable (Phadke *et al.* 2014), but can be affected by environmental conditions such as temperature and nutrition during sexual reproduction. The probabilistic SD was previously shown to cause the evolution of uneven sex ratios in natural populations of *T. thermophila* (Paixao *et al.* 2011).

Like most ciliates, *T. thermophila* are facultatively sexual: cells reproduce asexually by binary fission when food is abundant and conjugation, the non-reproductive sexual stage, is induced between cells of different sexes under starvation conditions (Orias *et al.* 2011) (Figure S1 in File S1). Each *T. thermophila* cell contains a diploid germinal micronucleus (MIC) and a polyploid somatic macronucleus (MAC). During conjugation, the MIC undergoes meiosis to form gamete nuclei that fuse to produce new zygotic MIC via reciprocal fertilization. The new MAC differentiates from mitotic copy of the new MIC and goes through developmental genome editing and polyploidization, and the old MAC is destroyed by programmed nuclear death. A recent study revealed that the B-type *mat* allele in the MIC contained six pairs of incomplete genes, specifying sex II-VII, respectively (Cervantes *et al.* 2013). During MAC development, all but one gene pair is deleted and the remaining pair are re-assembled at the MAC *mat* locus by joining to intact transmembrane (TM) exons that are shared across all sex gene pairs. After conjugation, progeny will go through a period of sexual immaturity, typically lasting for 40–80 asexual generations (Perlman 1973), during which time cells are unable to

mate. Knowledge about the patterns of probabilistic SD and molecular characterization of the *mat* allele makes *T. thermophila* a good multi-sex system in which to analyze the dynamics of sex ratio, from the perspective of population genetics.

Here, we first develop a population genetics model to dissect the mating kinetics in a large population of *T. thermophila* and to make quantitative predictions about how population sex ratio will evolve. We then investigate the impact of different parameters in the model on the dynamics of sex ratios. To test if population sex ratios follow the trajectories predicted by the model, we establish five replicate experimental populations and allow them to mate every 100 asexual generations, during which sex ratio dynamics and the frequencies of newly arisen mutations are tracked by time-course whole-genome sequencing. Overall, experimental observations highly support theoretical predictions. The newly established theoretical framework is applicable in principle to other multi-sex organisms and will provide more insight into the understanding of the maintenance of multiple sexes in natural populations.

Materials and Methods

The theory

Consider a large population of *T. thermophila*, in which sexual reproduction occurs periodically (for example, every 100 cell divisions) and in-between the population grows asexually.

Sexual reproduction starts with cell pairing (conjugation) which is assumed to be a random but synchronized process such that incompatible pairs (cells of the same sex) will dissolve and retry until no further pairing is possible. The process can be specified in detail as follows. Let p_i be the frequency of sex i right before the sexual reproduction and $q_i(t)$ be the relative frequency of sex i right after the t-th round of pairing, then $q_i(0) = p_i$. Since pairing is at random, at the t-th round of pairing the probability of a cell of sex i not paired is $q_i^2(t-1)$, and after the frequency is re-calibrated, the frequency of sex i among the unpaired cells is

$$q_i(t) = \frac{q_i^2(t-1)}{\alpha_t} \quad (1)$$

where $\alpha_t = \sum_i q_i^2(t-1)$, which is the expected relative proportion of unpaired cells after the t-th round of pairing. The overall proportion of unpaired cells will converge to

$$\alpha = \prod_{t=1} \alpha_t \quad (2)$$

which is necessarily all cells of the most frequent sex type (k) before the sexual reproduction starts. Table 1 presents a summary of this and other parameters used in the description of the sexual reproduction process. After recalibration, the percentage of sex i among the cells involved in the pairing is

$$(p_i - \delta_{i-k}\alpha)/(1-\alpha) \quad (3)$$

where δ_m takes value 1 if $m = 0$, and 0 otherwise.

In general not all paired cells proceed to the next step, some will dissolve and do not participate in the subsequent steps of the sexual reproduction together with the α proportion that are not paired. Let β represent the probability that each pair dissolves and furthermore it is assumed that each intact pair has probability γ to produce offspring (and has probability 1- γ to die without producing offspring). For each successfully reproducing pair, its two offspring have sex frequencies specified by the SD pattern $f = (f_1, \ldots, f_7)$. After the sexual reproduction, the total number of cells in the population is Nr where

$$r = \alpha + \beta(1-\alpha) + (1-\beta)(1-\alpha)\gamma \tag{4}$$

which is the probability that a cell either survives without participating in sexual reproduction or passes its genetics to offspring in sexual reproduction. Among the Nr cells, the proportion that is not sexual offspring is

$$[\alpha + \beta(1-\alpha)]/r \tag{5}$$

and there are

$$N\delta_{i-k}\alpha + N\beta(1-\alpha)(p_i - \delta_{i-k}\alpha)/(1-\alpha) + N(1-\beta)(1-\alpha)\gamma f_i \tag{6}$$

cells that are of sex i. Let $p_i^{'}$ be the frequency of sex i after the sexual reproduction. It follows that

$$\begin{aligned} p_i^{'} &= \frac{\delta_{i-k}\alpha + \beta(p_i - \delta_{i-k}\alpha) + (1-\beta)(1-\alpha)\gamma f_i}{r} \\ &= \frac{\beta p_i + (1-\beta)[\delta_{i-k}\alpha + (1-\alpha)\gamma f_i]}{r}. \end{aligned} \tag{7}$$

Since it is assumed that N is sufficiently large so that random genetic drift is negligible, $p_i^{'}$ will be the frequency of sex i right before the next round of sexual reproduction if there is no natural selection.

By setting $p_i^{'} - p_i = 0$, one can solve the equation for the equilibrium frequencies which lead to

$$p_i = \frac{\delta_{i-k}\alpha_\infty + (1-\alpha_\infty)\gamma f_i}{\alpha_\infty + (1-\alpha_\infty)\gamma} \quad (8)$$

where α_∞ is the limiting α value. It may appear that the equilibrium frequencies have nothing to do with β, but it is not true since its impact is reflected through the limiting α value.

Next we consider the impact of selectively advantageous mutations. Suppose a mutation emerges right after sex on a macronucleus of sex i with frequency $m_f^{'}$ and growth rate $1 + s$ per cell division. Then right before the next sexual reproduction, the proportions of cells of various sexes ($j = 1, \ldots, 7$) are

$$p_j = \frac{p_j^{'} + \delta_{i-j} m_f^{'}[(1+s)^n - 1]}{(1-m_f^{'}) + m_f^{'}(1+s)^n} \quad (9)$$

The frequency of cells containing the mutant right before sexual reproduction is

$$m_f = \frac{m_f^{'}(1+s)^n}{(1-m_f^{'}) + m_f^{'}(1+s)^n} \quad (10)$$

Immediately after the next sexual reproduction, mutant allele frequency becomes

$$m_f^{'} = \frac{\delta_{i-k}\alpha m_f / p_k + \beta(m_f - \delta_{i-k}\alpha m_f / p_k)}{r}$$

$$= \frac{\delta_{i-k}(1-\beta)\alpha / p_k + \beta}{r} m_f \quad (11)$$

where δ_{i-k} is 1 if the mutant (sex i) is the most frequent sex and 0 otherwise.

By substituting the m_f in Equation (11) by (10), it leads to

$$m_f^{''} = \frac{\delta_{i-k}(1-\beta)\alpha / p_k + \beta}{r} \frac{(1+s)^n}{(1-m_f^{'}) + m_f^{'}(1+s)^n} m_f^{'}$$

which leads to the equilibrium solution for $s > 0$

$$m_f^{'} = \left\{ \frac{\delta_{i-k}(1-\beta)\alpha / p_k + \beta}{r} (1+s)^n - 1 \right\} / ((1+s)^n - 1) \quad (12)$$

Apparently if α = 1, it will lead to the fixation of the mutant allele. Otherwise an internal equilibrium is possible.

If an advantageous mutation (in terms of growth) occurs in a micronuclear, and since the micronuclear is not expressed during growth, its advantage is hidden until it is passed to the macronuclear during sexual reproduction. The difference here is that the advantage is inheritable. Due to redistribution of sex, the mutant will spread over all sexes and eventually will be fixed without the necessity of fixing a sex.

The experiment

Design of the experiment: To develop a better understanding on how various factors may affect the fate of a population, and to test if sex ratio dynamics follows our theoretical predictions, five replicate experimental populations (CS1-CS5) were established, each started with induced mating between equal proportion of homogeneous ancestor cells of sex IV and VI. The resulting population grew asexually for 100 generations with stable but large population size achieved by daily serial transfer and then it went into the next round of sexual reproduction. This sex:asex cycle was repeated 10 times for each of the replicate experiments. Immediately before each starvation to induce sexual reproduction, a large sample of cells was extracted, of which a portion was stored in liquid nitrogen (Cassidy-Hanley 2012) and the remaining was used for whole-genome sequencing for mutation identification as well as the determination of sex ratio. Due to the high cost of the whole-genome sequencing, we only sequenced DNA samples from CS1-CS3 across all time points and CS4 from generation 400 to 1,000. Although samples from CS5 were not sequenced, it still provided useful information on what sex was eventually fixed

in the population. The essentials of the experiment are described below and more laboratory details can be found in the supplementary material (File S2).

Ancestral population: Strain SB210 mated with the star strain B*VII through genomic exclusion (GE) crosses (Allen 1967). The progeny of the GE crosses are whole-genome homozygotes in both nuclear genomes, but different progeny cells can exhibit different sexes in the MAC due to the probabilistic SD. When the progeny population matured, two cells, one of sex IV and another of sex VI (named Anc_IV and Anc_VI, respectively), were selected as ancestral cells and their asexual clonal populations became the starting cells for each of the replicate experimental populations. All these cells inherited the same B-type *mat* allele from SB210.

The parameters in the experimental populations: To estimate the parameters β and γ, only the proportional survival cells (a) and within which the proportion of asexual offspring (b) are required (when α is known). For example when $\alpha = 0$, it follows from (4) and (5) that $\beta = \mathrm{a} \times \mathrm{b}$ and $\gamma = \beta \times (1 - b)/[b \times (1 - \beta)]$. The sex ratio pattern of the evolving population at the end of the first sex:asex cycle (i.e. at generation 100) was used to estimate f. As unmated Anc_IV and Anc_VI cells underwent serial passage along with progeny produced by sexual reproduction, correction for the background sex ratio of unmated cells was necessary to obtain the true f value representing the sex ratio pattern of sexual progeny. In addition, because natural selection during serial passage will also affect the estimation of f, we therefore recorded the daily growth rate as $\ln\left(\frac{\text{cell density\_24hr}}{\text{cell density\_0hr}}\right)/24$ (Kishimoto *et al.* 2010) of the two ancestral populations in a week before mating and the resulting

252 population during the following 100 asexual generations. For each evolving
253 population, we tracked the changes in fitness by measuring the growth rate and
254 determined parameter *s* as the ratio (minus 1) of the eventual population fitness and
255 the starting ancestral population fitness that was calculated as the mean growth rate
256 of the two ancestral populations over the week of serial passage. The relative fitness
257 trajectory of each evolving population was analyzed by the SSlogis model in R 3.4.1
258 (http://www.r-project.org/).
259
260 **Determination of sex ratio and identification of sexual progeny:** The sex ratios in
261 each sample were determined by mapping sequencing reads to the MIC reference
262 genome (Hamilton *et al.* 2016). After removing the internally eliminated sequences
263 (IESs) background within the *mat* locus, the sequencing depth of gene segments
264 specific to each sex was used to determine the proportion of each sex. Two different
265 approaches were used to determine whether unmated ancestral cells were
266 responsible for the fixed sex. First, we performed sex testing experiments for all
267 evolving populations at generation 600. Each evolving population was mixed
268 separately with cultures of six test strains that are of sex II–VII, respectively
269 (Hamilton and Orias 2000) to determine its fixed sex. Second, we used SNPs in the
270 TM and truncated transmembrane (tm) exons of the MIC *mat* locus as molecular
271 makers to distinguish sexual progeny from unmated ancestral cells because sexual
272 progeny can acquire novel combinations of SNPs into MAC TM exons during mating
273 (see details in File S2).
274

Whole genome sequencing, SNP calling and annotation: To track sex ratio dynamics and analyze the SNP in MAC TM exons to distinguish between sexual progeny and unmated ancestral cells, DNA samples were taken from populations CS1, CS2 and CS3 every 100 asexual generations until generation 1000. For SNP analysis in MAC TM exons in the population CS4, DNA samples were taken every 100 asexual generations from generation 400 to 1000. To prevent possible changes to the genetic structure of populations resulting from long-term storage, all DNA samples were isolated as soon as taken from each evolving population. However, due to the poor quality of the DNA sample from the CS2 population at generation 200, cell stock in liquid nitrogen was thawed and used for DNA isolation. Sequencing libraries were constructed using a standard Illumina protocol as previously described (Xiong *et al.* 2015). All libraries were sequenced to depths of about 30-fold coverage except libraries of the two ancestral samples that were sequenced to ~250-fold coverage, using Illumina HiSeq 2000 or HiSeq 2500 instruments. A detailed SNP calling pipeline is given in File S2. Briefly, sequenced reads after trimming off adapters were aligned to *T. thermophila* MAC reference genome (Stover *et al.* 2006). Then we marked PCR duplicate reads, performed local realignment around potential indels and recalibrated the base quality score. We next ran VarScan 2.3.9 (Koboldt *et al.* 2009; Koboldt *et al.* 2012) for SNP calling. To reduce the risk of false positives, each mutation had to be supported by at least three forward and three reverse reads as previously reported (Sung *et al.* 2012; Long *et al.* 2016). By taking advantage of our time-course sequencing, we further refined candidate mutations based on mutation frequency trajectories, as previously reported (Lang *et al.* 2013; McDonald *et al.* 2016). In particular, the imprecise IES excision in the newly developing MAC during

299 mating can result in the formation of many SNPs or indels around the IES junction
300 sites (Hamilton *et al.* 2016). Therefore, candidate mutations were required to be
301 located at least 60bp from the IES excision endpoint. Functional annotation of each
302 mutation was carried out using SnpEff (Cingolani *et al.* 2012).
303
304 **Identification and functional validation of beneficial mutations:** We used two
305 criteria to identify putative beneficial mutations. First, beneficial mutations are more
306 likely than neutral or deleterious mutations to spread within a population. Thus, we
307 considered mutations that reached a frequency of at least 0.9 as candidate beneficial
308 mutations. Second, the frequency of beneficial mutations should correlate with
309 changes in fitness. We therefore determined the Pearson correlation coefficients
310 between changes in fitness and the frequency of each identified mutation. Putative
311 beneficial mutations were required to have a correlation coefficient of ≥+0.8 (Table
312 S2). Mutations that met both criteria were classified as beneficial. To validate
313 whether a selected mutation confers a fitness benefit, we introduced it into both
314 ancestral cells, see supplementary material in File S2. Then we mixed each mutant
315 cell population with its corresponding ancestral cell population in roughly equal
316 proportion and propagated them under the same conditions as the evolution
317 experiment. Sanger sequencing was performed every two days to determine the
318 relative proportion of each cell type. PCR primers used to amplify sequences contain
319 mutation site were: Mut-f4001 5'-TAGATTAAGACACTTTAGAAAAAGC-3' and Mut-
320 r4898 5'-TCATTGATTCATTAGATTATCTTTC-3'. Competition assays were carried out in
321 duplicate.
322

Data availability

The mathematic model was analyzed using Java 9 and the source code will be available upon request. File S1 contains additional figures including the life cycle of *T. thermophila* (Figure S1), impact of the model parameters on sex ratio patterns when using another f (Figure S2), and growth rate records of the two ancestral populations and the three sequenced evolving population during the first 100 asexual generations (Figure S3). Table S1 in File S1 shows the sex ratios in the three sequenced evolving populations at generation 100. File S2 contains additional Materials and Method sections. Table S2 contains frequency trajectories and functional annotation of all identified mutations. Supplementary material has been uploaded to figshare. All genome sequencing data are available at Sequence Read Archive with accession number SRP080979.

Numerical Results

Impact of the model parameters on the equilibrium frequencies of sexes

As shown in the Theory section, parameters influencing the equilibrium sex ratios include the initial population sex ratio before mating, β, γ, f and s. We thus explored numerically the impact of these parameters.

Define f_{max} as the largest f_i and sf_{max} as the corresponding sex. To simplify the illustration, we first set f to be the estimated SD pattern (II, 0.306; III, 0.010; IV, 0.267; V, 0.047; VI, 0.113; VII, 0.257) from our experiments. Then, $f_{max} = 0.306$ and $sf_{max} = \mathrm{II}$. We started by considering the scenario in which the population starts with two randomly selected sexes of equal proportions (Figure 1, A-D). Figure 1A shows that the population sex ratios at equilibrium exhibit two patterns under

different combinations of β and γ: all six sexes co-exist or a single sex is fixed. Specifically, larger γ facilitates the co-existence, and the probabilities of fixing different sexes are positively correlated with the sex frequency distribution in f. In addition, Figure 1, B-D indicates larger β can increase the probability of fixing other sexes except the sf_{max}. We then allowed in the initial population random sex ratio of the given set of sexes (but their frequencies sum necessarily to 1). Figure 1E shows that random sex ratio remarkably decreases the fixation probability of f_{max} compared to that shown in Figure 1A. However, increasing the number of sexes in the initial population promotes the fixation of f_{max} (Figure 1F). These comparisons show that higher sex diversity, including more even sex ratio and greater number of sexes, facilitates the fixation of f_{max}. In the extreme case, when a population starts with equal proportions of all the six sexes, only the sf_{max} (sex II) can be fixed (Figure 1G). Similar results were also found when f is set to other SD patterns, such as the one described in the Introduction section (Figure S2 in File S1).

Next, we evaluated the impact of f_{max} values on the patterns of equilibrium sex ratios. For a B-type *mat* allele, the f_{max} value can range from 1/6 to 1. Figure 1H shows the probability of co-existence of all sexes decreases with the increase of f_{max}. In particular, when f_{max} is greater than 0.5, co-existence will not occur. A simple explanation is that when more than half of the progeny produced by any two of the six sexes in a random-mating population express the sex of f_{max}, the frequency of f_{max} will gradually increase up to fixation.

We further investigated how mutation that occurs on the MAC right after sexual reproduction affects the evolutionary consequence of sex ratios. For simplicity, we only considered the two cases in which either the sf_{max} (sex II, Figure 2A) or the

371 least frequent one (sex III, Figure 2B) obtains a beneficial mutation, and assumed
372 that the population starts with equal proportions of any two of the six sexes.
373 Compared to Figure 1A, Figure 2 shows that the patterns of equilibrium sex ratio
374 changes strikingly. Sex obtaining a beneficial mutation has an increased probability
375 to be fixed and larger β or *s* values will intensify this tendency. When *s* is larger than
376 a certain threshold, sex with the beneficial mutation will be destined for fixation
377 regardless of the values of β and γ.
378
379 **Impact of environmental fluctuations on the equilibrium frequencies of the sexes**
380 In the numerical exploration described above, f is fixed which is relatively
381 stable for a given experimental setting. However, in reality change in some
382 environmental factors may lead to the modification in the values of f and other
383 parameters. In natural populations of *T. thermophila*, a series of environmental
384 fluctuations including the changes of abiotic and biotic factors are possible to
385 influence the equilibrium sex ratio pattern that has already established in the ideal
386 mating population. For example, migration among populations leads to the
387 immediate changes of population sex ratio, temperature and food availability affect
388 the parameter f (Nanney 1960; Orias and Baum 1984) and a salty environment can
389 changes the values of β and γ.
390 For simplicity of illustration, consider a population in which cells will not
391 dissolve once successfully paired together ($\beta = 0$) and all pairs will produce progeny
392 ($\gamma = 1$), its sex ratio at equilibrium can be readily predicted when the parameter f is
393 determined. For example, a population with the empirically estimated f will reach
394 the following equilibrium sex ratio: II, 0.316; III, 0.010; IV, 0.263; V, 0.046; VI, 0.112;

VII, 0.253. By imposing a varying degree of deviations or fluctuations on either the established equilibrium sex ratio (Figure 3A) or the parameter f when determining the progeny sex distribution after each round of mating (Figure 3B), we found sex ratio patterns are both changed dramatically and the impact of fluctuation on parameter f seems more remarkable. A slight fluctuation will lead first to the fixation of the f_{max}, and with the increase of fluctuation degrees, other sexes can also be fixed with probabilities positively correlated with the sex frequency distribution in f.

Experimental results

Parameter estimation and prediction of sex ratio dynamics

After mating between the two ancestral populations of equal proportion ($\alpha = 0$), we found in the five replicate experimental populations, the number of cells decreased to an average of 52% within which 38% were the two unmated ancestral cells and each of them should account for 19%. According to equation (4) and (5), parameter β is equal to 20%, and γ is equal to 40%. As there was no significant difference in growth rate among the two ancestral populations and the resulting population after mating (Figure S3 in File S1), it is reasonable to assume that the proportion of each unmated ancestral cell (19%) did not change significantly and the effect of natural selection could be neglected during serial passage for the first 100 generations. Thus, after correction by subtracting background sex ratio of unmated ancestral cells from the average sex ratio (Table S1 in File S1) in the three sequenced evolving populations (CS1-CS3) at generation 100, the f values were: II, 0.306; III, 0.010; IV, 0.267; V, 0.047; VI, 0.113; VII, 0.257.

419 Using these estimated parameter values, we could readily predict the sex ratio
420 dynamics in a large experimental population. When a population begins with the two
421 ancestral populations in equal proportions and mates every 100 asexual generations,
422 and there is no selection, we found sex II would increase in frequency gradually and
423 eventually be fixed (Figure 4B).
424
425 **Natural selection is responsible for the fixation of single sex**
426 Sex ratio dynamics showed that at generation 100, all three sequenced populations
427 (CS1-CS3) contained a mixture of cells with sex II–VII. Over time, however, a different
428 single sex became dominant gradually and then fixed within each population (Figure
429 5A). In addition, during each round of mating, we calculated the ratios of mating
430 pairs and sexual progeny (File S2). After several sex:asex cycles, no mating pairs or
431 sexual progeny were observed in any of the replicate populations (Table 2). Sex
432 testing at generation 600 showed that each population expressed only a single sex,
433 but there were four different sexes fixed in the five replicate populations. These
434 results deviated strikingly from the prediction that only sex II could be fixed if all
435 parameters were the same and there is no selection. Considering the large
436 population size in our experiment, the observed deviations are unlikely to be caused
437 by genetic drift. A more plausible explanation is that a subgroup of cells expressing a
438 specific sex gain an increased growth fitness and expanded to fixation consequently.
439 Indeed, the overall growth record revealed that the relative fitness of each evolving
440 population increased markedly (Figure 5B).
441 In three of the replicate populations (CS1, CS2, and CS4), the fixed sexes were
442 the same as one of the ancestral cells, sex IV or VI. However, according to SNP

443 analysis in the MAC TM exons, we identified several SNPs that were either lost or
444 became fixed in each of the three populations (Figure 5C). In addition, the other two
445 populations, CS3 and CS5, fixed different sexes (II and VII, respectively) than the
446 ancestral cells. Thus, unmated ancestral cells had been completely replaced in all the
447 five replicate populations, suggesting that sexual progeny cells might gain a faster
448 growth rate than ancestral cells.
449
450 **Identification of beneficial mutations**
451 The analysis described in the previous section establishes that increased fitness of
452 sexual progeny was responsible for the fixation of a certain sex in each of the
453 replicate populations. To reveal the molecular basis underlying the increased fitness,
454 we turn to whole-genome sequencing data. We detected an average of 14.7 *de novo*
455 mutations per population and several candidate beneficial mutations were identified
456 in the three sequenced populations: two in CS1, one in CS2, and one in CS3. We then
457 investigated whether a selected candidate beneficial mutation from the CS1
458 population confers a fitness benefit (Figure 6A; red line). This point mutation
459 resulted in a premature termination codon in a gene encoding a serine/threonine
460 kinase (Table S2). Within 12 days, ancestral cells had been completely replaced by
461 mutant cells (Figure 6B), providing clear evidence that the selected mutation
462 conferred increased growth fitness.
463 Given that genes determining sexes are not expressed during growth, it seems
464 unlikely that they can confer a selective advantage leading to their own rapid fixation.
465 However, in the case of the CS1 population, purification of sex IV preceded the
466 fixation of all candidate beneficial mutations. This apparent paradox might be

467 explained in the following way: directly after a single sex becomes purified, the
468 population might still contain two different cell types of the same sex, with only one
469 of these containing a beneficial mutation. In the CS1 population, sex IV had become
470 purified by about generation 500 (Figure 6A; green line). However, the novel SNP at
471 MAC *mat* locus, a marker for the eventually fixed sex IV genes, did not become fixed
472 until about generation 600 (Figure 6A; purple line). This suggested that not all MAC
473 *mat* loci exhibiting sex IV contained this novel SNP at generation 500, and that over
474 the following 100 asexual generations (from generation 500 to 600), those sex IV
475 cells containing the novel SNP swept rapidly to fixation by outcompeting sex IV cells
476 lacking the novel SNP, a phenomenon known as “clonal interference”. Notably,
477 frequency changes in the novel SNP and the verified beneficial mutation correlated
478 strongly (r = 0.99). This result suggested that sex IV cells containing the novel SNP
479 also acquired this verified beneficial mutation, and sex IV genes within the cells
480 became fixed through genetic hitchhiking with the beneficial mutation.

481 Moreover, the effect of selection due to newly arisen beneficial mutations was
482 likely to be the cause that trajectories of sex ratio in experimental populations
483 deviated strikingly from theoretical prediction that assumed no selection. According
484 to the fitness trajectories, the values of s in three sequenced populations are: 0.12 in
485 CS1, 0.10 in CS2, 0.14 in CS3. For each population, we then assumed a mutated cell
486 expressing the fixed sex acquired the corresponding selective advantage in the MAC
487 right after one of the first five rounds of mating, respectively. In fact, we did not
488 detect the verified beneficial mutation of the CS1 population in the MIC sequencing
489 data (data not shown). The results showed the predicted frequency trajectory of the
490 fixed sex could highly agree with the observation for each population under a

491 specific assumption (Figure 6C). The relative low agreement in the CS2 population
492 might have resulted from a DNA sample at generation 200 being isolated from the
493 thawed cultures stored in liquid nitrogen, and the long-term storage might change
494 the composition of population sex ratio. Overall, when considering the effect of
495 selection, the results showed that the experimental observations highly supported
496 our model's predictions and newly arisen beneficial mutations were the cause of the
497 fixation of single sexes in the populations. In addition, the agreement between
498 experimental observations and model predictions in the three sequenced
499 populations (CS1-CS3) suggested that the fixation of a single sex in the populations
500 CS4 and CS5 was also probably due to newly arisen beneficial mutations because
501 both of these two populations showed a remarkably increased growth fitness (Figure
502 5B) and fixed a different sex (IV and VII, respectively) than sex II that is predicted to
503 be the only fixed sex when there is no selection (Figure 4).
504

505 **Discussion**

506 In organisms with two sexes, male and female, the strategy to adjust population sex
507 ratio has been well demonstrated. Nonetheless, how organisms with multiple sexes
508 maintain proper sex ratio in the population remains poorly understood. Based on a
509 newly developed population genetics model, we analyzed in this study the dynamics
510 of population sex ratio in *T. thermophila*, a ciliate with seven sexes and probabilistic
511 SD mechanism. We found there are plenty opportunities for both the co-existence of
512 all sexes and the fixation of a single sex, depending on the combinations of several
513 parameters, including the strength of natural selection. Specifically, parameter γ
514 mainly determines which pattern the population will exhibit, and the probability that

515 a specific sex is fixed is positively correlated with its frequency in parameter f, but it
516 is also affected by β (Figure 1, B-D). Natural selection can strongly shift the sex ratio
517 pattern toward the fixation of a single sex with a growth advantage. Moreover, in
518 natural populations of *T. thermophila*, all of these parameters likely fluctuate along
519 with changing environmental conditions, which can further diversify the population
520 sex ratio patterns (Figure 3). Experimental observations of sex ratio dynamics
521 confirmed the validity of the model's predictions.

522 In natural habitats of *T. thermophila*, all seven sexes were generally present
523 (Doerder *et al.* 1995). However, sex ratios varied remarkably in different sampled
524 ponds and even displayed local and seasonal variation in the same pond. It was
525 postulated that sex ratio variations between and within ponds are due to the
526 fluctuations of SD pattern through the interaction between multiple *mat* alleles and
527 environmental conditions (Arslanyolu and Doerder 2000). This hypothesis is
528 consistent with our model prediction that there is sufficient opportunities for the co-
529 existence of all seven sexes and environmental fluctuations can further increase the
530 diversity of sex ratios. Moreover, it suggests that population sex ratios at equilibrium
531 are determined by not only the SD pattern f but also other parameters involved in
532 sexual reproduction (equation 9). Thus, our theoretical model provides a
533 comprehensive framework to illustrate how natural populations of *T. thermophila*
534 maintain proper sex ratios when responding to changeable environments.

535 Our numerical exploration also suggests that there is a large probability of
536 fixation of a single sex in a local population. Indeed, due to limited rates of dispersal
537 in *T. thermophila* (Zufall *et al.* 2013), local populations or subpopulations sampled
538 from the same pond often contained only a single sex even though all sexes are

present in the pond (Doerder *et al.* 1995). The fixation of a single sex in a location can potentially provide an advantage to prevent inbreeding because a particular consequence of probabilistic SD is that it allows for mating among genetically identical individuals at the micronucleus. The experimental results combined with the model's predictions suggest that the fixation of a single sex is often caused by beneficial mutations during sexual reproduction. Interestingly, the process of choosing which sex to be fixed seems to be random because four different sexes are fixed in the five replicate experimental populations. Thus, it is likely that in natural subpopulations, the spontaneous beneficial mutations help their carrying sex to fixation, which effectively blocks further local inbreeding, and then the subpopulations can expand rapidly through asexual production. However, due to the probabilistic SD, mating between subpopulations only containing two different sexes could lead to the recovery of all the seven sexes, which facilitates the population to regain the benefits provided by sex when the environment changes dramatically. Thus, the particular probabilistic SD may provide an advantageous mechanism for the lineage survival of *T. thermophila* by allowing this species to integrate the benefits of both sexual and asexual reproduction. However, why the number of sexes is fixed at seven in natural populations of *T. thermophila* remains a mystery. In fact, the *Tetrahymena* species have various number of sexes ranging from three to nine and display different modes of sexual inheritance (Phadke and Zufall 2009), but little is known about their SD mechanisms, which needs further sequencing of the MIC genome to elucidate. When more SD mechanisms and sex ratio data from experimental evolution and natural populations in different species are available, comparative analysis may be used to explore if there exists an optimal number of sex

563 for a specific species to adjust sex ratio dynamics in the light of our theoretical
564 framework.

565 In summary, our theoretical model combined with experimental results
566 provides a comprehensive framework to analyze the dynamics of sex ratio in *T.*
567 *thermophila*, and proposes a possible strategy of maintaining multiple sexes in
568 natural populations of *T. thermophila*. In principle, the newly established theoretical
569 framework is applicable to other multi-sex organisms to bring additional insight into
570 the understanding of maintenance of multiple sexes in a natural population.

571

572

573 **Acknowledgments**

574 We thank Eduardo Orias (University of California Santa Barbara) and Yong Zhang
575 (Institute of Zoology, Chinese Academy of Sciences) for helpful discussions during the
576 study. Additional students in Miao's laboratory provide assistance in the long-term
577 cell culture: Wentao Yang, Guanxiong Yan, Zongyi Sun, and Chuanqi jiang. This study
578 was supported by the National Natural Science Foundation of China (grant number
579 91631303 to W.M. and 91631304 to Y.X.F).

580

581

582

583

584

585

586

Literature Cited

Allen S. L., 1967 Genomic exclusion: a rapid means for inducing homozygous diploid lines in *Tetrahymena Pyriformis,* syngen 1. *Science* **155:** 575-577.

Ammermann D., 1982 Mating Types in *Stylonychia mytilus* Ehrgb. *Archiv für Protistenkunde* **126:** 373-381.

Arslanyolu M., Doerder F. P., 2000 Genetic and environmental factors affecting mating type frequency in natural isolates of *Tetrahymena thermophila*. *J. Euk. Microbiol.* **47:** 412-418.

Bell G., 1982 *The masterpiece of nature: the evolution and genetics of sexuality*. University of California Press, Berkeley.

Burt A., 2000 Perspective: sex, recombination, and the efficacy of selection - was Weismann right? *Evolution* **54:** 337-351.

Cassidy-Hanley D. M., 2012 *Tetrahymena* in the laboratory: strain resources, methods for culture, maintenance, and storage. *Methods Cell. Biol.* **109:** 237-276.

Cervantes M. D., Hamilton E. P., Xiong J., Lawson M. J., Yuan D. X. *et al.*, 2013 Selecting one of several mating types through gene segmentjoining and deletion in *Tetrahymena thermophila*. *PLoS Biol.* **11:** e1001518.

Cingolani P., Platts A., Wang L. L., Coon M., Nguyen T. *et al.*, 2012 A program for annotating and predicting the effects of single nucleotide polymorphisms, SnpEff: SNPs in the genome of *Drosophila melanogaster* strain w1118; iso-2; iso-3. *Fly* **6:** 80-92.

609 Doerder F. P., Gates M. A., Eberhardt F. P., Arslanyolu M., 1995 High frequency of sex
610 and equal frequencies of mating types in natural populations of the ciliate
611 *Tetrahymena thermophila*. *Proc. Natl. Acad. Sci. USA* **92:** 8715-8718.
612 Fisher R. A., 1930 *The genetical theory of natural selection*. Clarendon Press, Oxford,.
613 Hamilton E. P., Orias E., 2000 Genetic crosses: setting up crosses, testing progeny,
614 and isolating phenotypic assortants. *Methods Cell. Biol.* **62:** 219-228.
615 Hamilton E. P., Kapusta A., Huvos P. E., Bidwell S. L., Zafar N. *et al.*, 2016 Structure of
616 the germline genome of *Tetrahymena thermophila* and relationship to the
617 massively rearranged somatic genome. *Elife* **5:** e19090.
618 Kishimoto T., Iijima L., Tatsumi M., Ono N., Oyake A. *et al.*, 2010 Transition from
619 positive to neutral in mutation fixation along with continuing rising fitness in
620 thermal adaptive evolution. *PLoS Genet.* **6:** e1001164.
621 Koboldt D. C., Chen K., Wylie T., Larson D. E., McLellan M. D. *et al.*, 2009 VarScan:
622 variant detection in massively parallel sequencing of individual and pooled
623 samples. *Bioinformatics* **25:** 2283-2285.
624 Koboldt D. C., Zhang Q., Larson D. E., Shen D., McLellan M. D. *et al.*, 2012 VarScan 2:
625 somatic mutation and copy number alteration discovery in cancer by exome
626 sequencing. *Genome Res.* **22:** 568-576.
627 Lang G. I., Rice D. P., Hickman M. J., Sodergren E., Weinstock G. M. *et al.*, 2013
628 Pervasive genetic hitchhiking and clonal interference in forty evolving yeast
629 populations. *Nature* **500:** 571-574.
630 Long H. A., Winter D. J., Chang A. Y. C., Sung W., Wu S. H. *et al.*, 2016 Low base-
631 substitution mutation rate in the germline genome of the ciliate *Tetrahymena*
632 *thermophila*. *Genome Biol. Evol.* **8:** 3629-3639.

McDonald M. J., Rice D. P., Desai M. M., 2016 Sex speeds adaptation by altering the dynamics of molecular evolution. *Nature* **531:** 233-236.

Muller H. J., 1932 Some genetic aspects of sex. *Am. Nat.* **66:** 118-138.

Nanney D. L., 1960 Temperature effects on nuclear differentiation in variety 1 of *Tetrahymena pyriformis*. *Physiol. Zool.* **33:** 146-151.

Orias E., Baum M. P., 1984 Mating type differentiation in *Tetrahymena thermophila*: strong influence of delayed refeeding of conjugating pairs. *Dev. Genet.* **4:** 145-158.

Orias E., Cervantes M. D., Hamilton E. P., 2011 *Tetrahymena thermophila*, a unicellular eukaryote with separate germline and somatic genomes. *Res. Microbiol.* **162:** 578-586.

Orias E., Singh D. P., Meyer E., 2017 Genetics and epigenetics of mating type determination in *Paramecium* and *Tetrahymena*. *Annu. Rev. Microbiol.* **71:** 133-156.

Paixao T., Phadke S. S., Azevedo R. B. R., Zufall R. A., 2011 Sex ratio evolution under probabilistic sex determination. *Evolution* **65:** 2050-2060.

Perlman B. S., 1973 Temperature effects on maturity periods in *Tetrahymena Pyriformis* Syngen 1. *J. Protozool.* **20:** 106-107.

Phadke S. S., Zufall R. A., 2009 Rapid diversification of mating systems in ciliates. *Biol. J. Linn. Soc.* **98:** 187-197.

Phadke S. S., Paixao T., Pham T., Pham S., Zufall R. A., 2014 Genetic Background alters dominance relationships between *mat* alleles in the ciliate *Tetrahymena thermophila*. *J. Hered.* **105:** 130-135.

Speijer D., Lukes J., Elias M., 2015 Sex is a ubiquitous, ancient, and inherent attribute of eukaryotic life. *Proc. Natl. Acad. Sci. USA* **112:** 8827-8834.

Stover N. A., Krieger C. J., Binkley G., Dong Q., Fisk D. G. *et al.*, 2006 *Tetrahymena* Genome Database (TGD): a new genomic resource for *Tetrahymena thermophila* research. *Nucleic. Acids. Res.* **34:** D500-D503.

Sung W., Tucker A. E., Doak T. G., Choi E., Thomas W. K. *et al.*, 2012 Extraordinary genome stability in the ciliate *Paramecium tetraurelia*. *Proc. Natl. Acad. Sci. USA* **109:** 19339-19344.

Weismann A., 1887 On the signification of the polar globules. *Nature* **36:** 607-609.

West S. A., 2009 *Sex allocation*. Princeton University Press, Princeton and Oxford.

Xiong J., Wang G. Y., Cheng J., Tian M., Pan X. M. *et al.*, 2015 Genome of the facultative scuticociliatosis pathogen *Pseudocohnilembus persalinus* provides insight into its virulence through horizontal gene transfer. *Sci. Rep.* **5:** 15470.

Zufall R. A., Dimond K. L., Doerder F. P., 2013 Restricted distribution and limited gene flow in the model ciliate *Tetrahymena thermophila*. *Mol. Ecol.* **22:** 1081-1091.

679 ## Figure legends

680 **Figure 1. Impact of the model parameters on sex ratio patterns when there is no**
681 **selection.** (A-D) Sex ratio pattern at equilibrium when the population starts with
682 equal proportions of any two of the six sexes (A) and under three specific β values
683 (B-D). The gray color represents the situation that all sexes co-exist and the other six
684 colors represent the fixation of one of the six sexes II-VII, respectively. The color
685 gradients represent the probability of occurrence for each situation. This color
686 scheme applies to all panels except panel H. (E,F) Sex ratio patterns at equilibrium
687 when the population starts with any two of the six sexes (E) or all the six sexes (F)
688 and the initial sex ratio is random but the sum is 1. (G) A special case of sex ratio
689 pattern when the population starts with even proportions of six sexes. (H) The
690 probability of co-existence of the six sexes under different values of f_{max}, the most
691 frequent sex in parameter f and β is set to 0.

692

693 **Figure 2. Impact of selection on sex ratio patterns. Sex ratio pattern at equilibrium**
694 **when sex II, the most frequent sex.** (A) and sex III, the least frequent sex (B) in
695 parameter f obtain a beneficial mutation with different selective coefficients. Color
696 regime is the same as Figure 1A.

697

698 **Figure 3. Impact of environmental fluctuations on sex ratio patterns. Sex ratio**
699 **pattern at equilibrium when the established equilibrium sex ratio.** (A) or the
700 empirically estimated parameter f (B) fluctuates with varying degrees. Color regime
701 is the same as Figure 1A.

702

703 **Figure 4. Prediction of sex ratio dynamics.** Predicted sex ratio trajectory when
704 populations start with equal proportions of the two ancestral populations and mate
705 every 100 asexual generations, and there is no selection.
706
707 **Figure 5. Increased fitness of sexual progeny were responsible for the fixation of a**
708 **certain sex in each of the replicate populations.** (A) Sex ratio dynamics in the
709 populations CS1 to CS3. Each colored bar represents the frequency of a sex, as
710 determined by sequencing data. (B) Relative fitness trajectories during experimental
711 evolution. The fitted growth model for each replicate population was plotted with a
712 different colored line. (C) Temporal changes in the frequency of novel SNPs
713 recombined into progeny MAC TM exons. Panels show SNP frequency changes in the
714 CS1, CS2, and CS4 populations. Numbers indicate SNP positions at the MIC *mat* locus
715 and frequency changes refer to non-reference bases, e.g. in the CS1 panel, for A > C,
716 A is the reference base and C is the non-reference base. Generation 0 represents
717 SNP frequency in the two ancestral cells. Each SNP is represented by the same color
718 in all three panels.
719
720 **Figure 6. The fixation of a single sex in the population is caused by newly arisen**
721 **beneficial mutations.** (A) Interactions between beneficial mutations and sex fixation
722 in the CS1 population. Red line, a verified beneficial mutation; gray lines, other
723 detected mutations. The green shows the process of sex IV purification within the
724 population. The black line shows the growth fitness trajectory. The purple line
725 represents the change in frequency of the fixed novel SNP at the MAC *mat* locus
726 (shown in Figure 5C; purple line in CS1). (B) Functional validation of putative

beneficial mutations. Each of ancestral cell populations was co-cultured with its corresponding mutant cell population containing the candidate beneficial mutation (panel A; red line) with daily serial passage. DNA samples were taken every 2 days and analyzed by Sanger sequencing to determine the relative ratio of the two cell types. Competition assays were performed in duplicate. (C) Comparison of sex fixation trajectories between experimental observations and the model's predictions. Model predictions assume the fixed sex in each population acquired a beneficial mutation in the MAC after one of the first five rounds of mating. Black dots are observed frequencies. The best fits are shown as red lines.

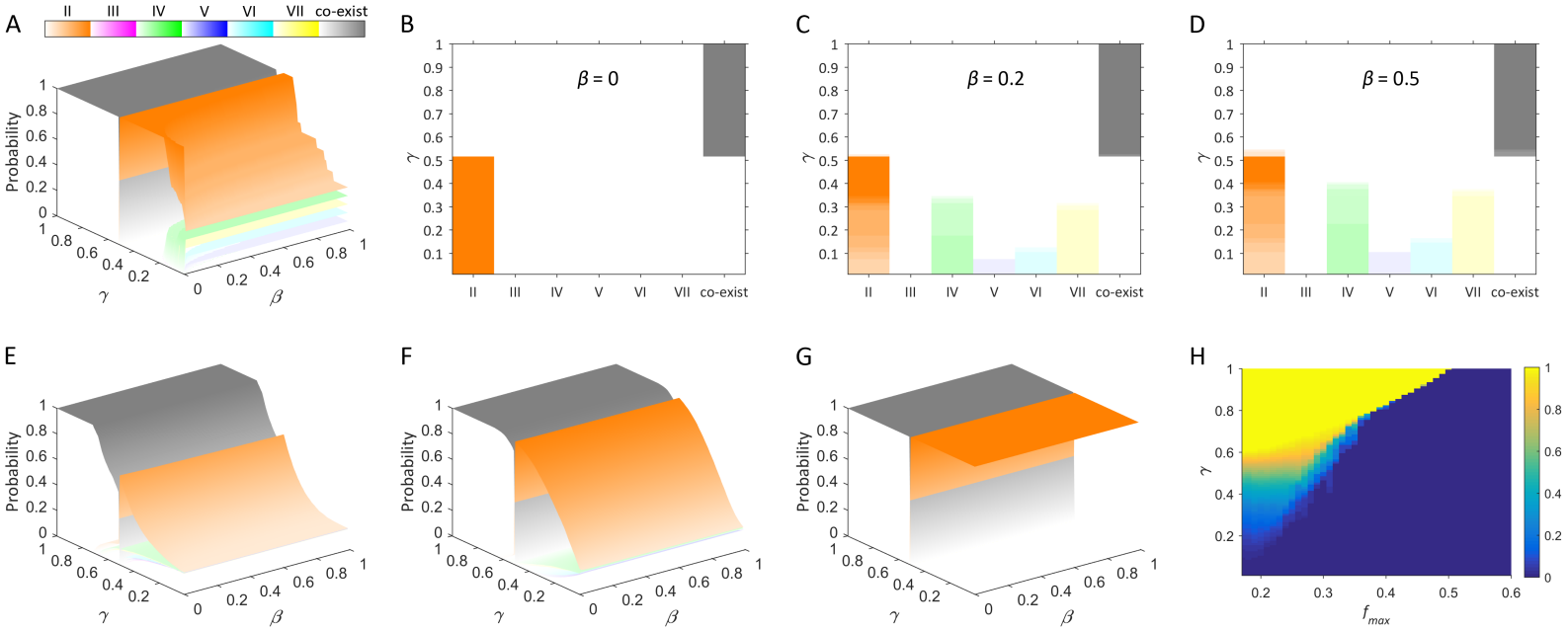
A
II III IV V VI VII co-exist
Probability
γ
β
B
β = 0
C
β = 0.2
D
β = 0.5
E
F
G
H
f_{max}

A

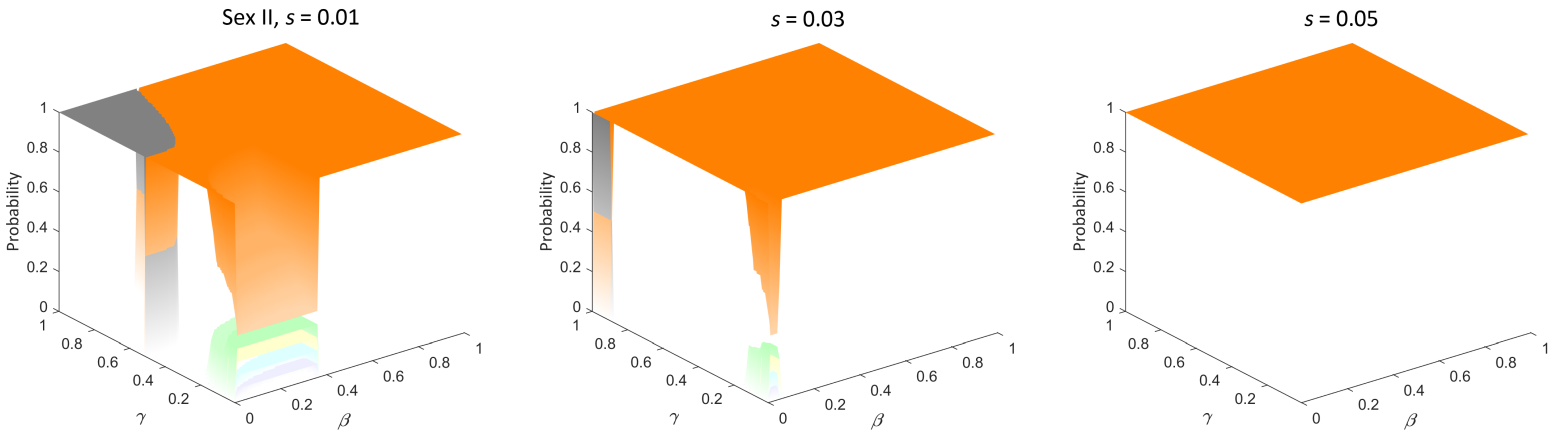
Sex II, s = 0.01
s = 0.03
s = 0.05
Probability
γ
β

B

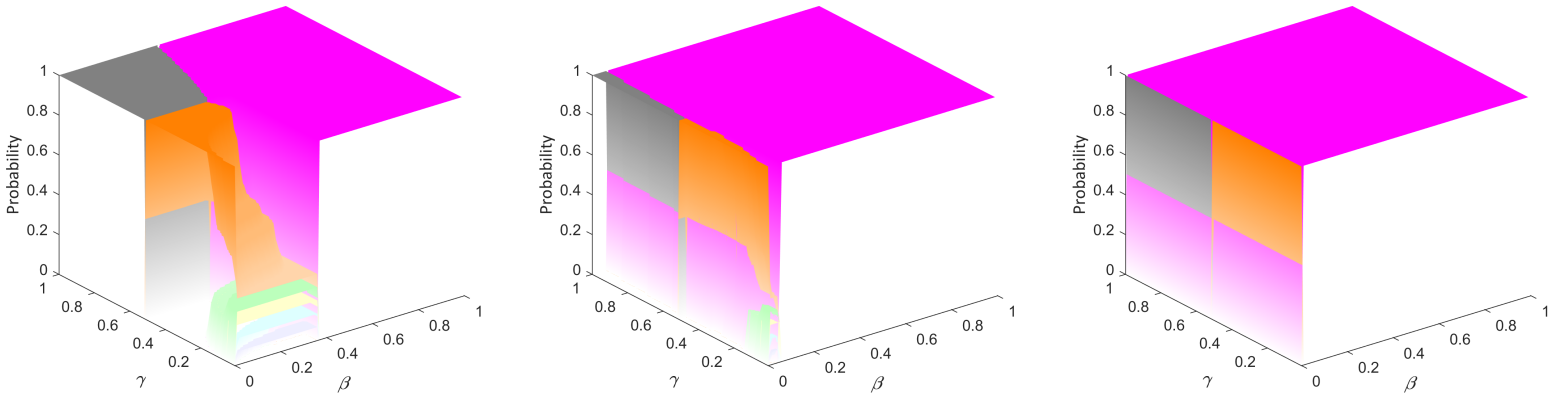
Sex III, s = 0.01
s = 0.03
s = 0.05
Probability
γ
β

A

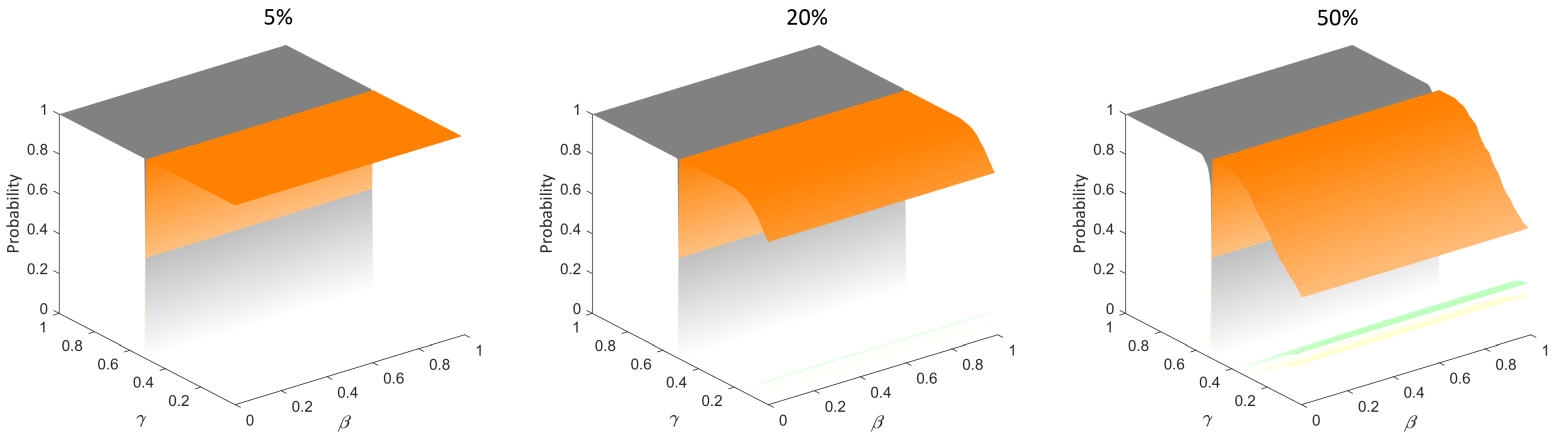

B

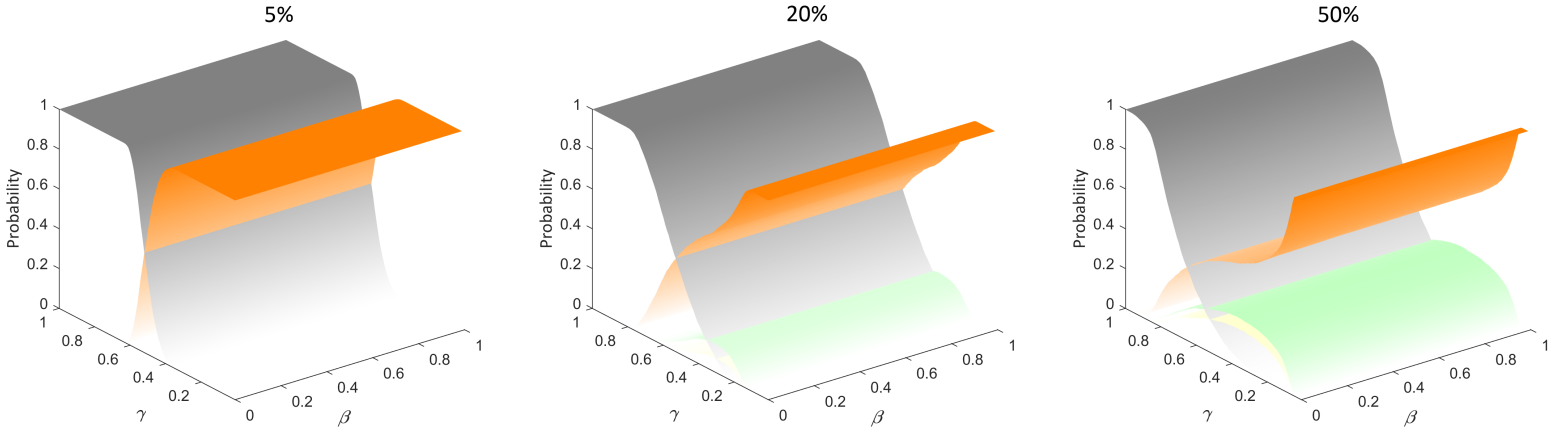

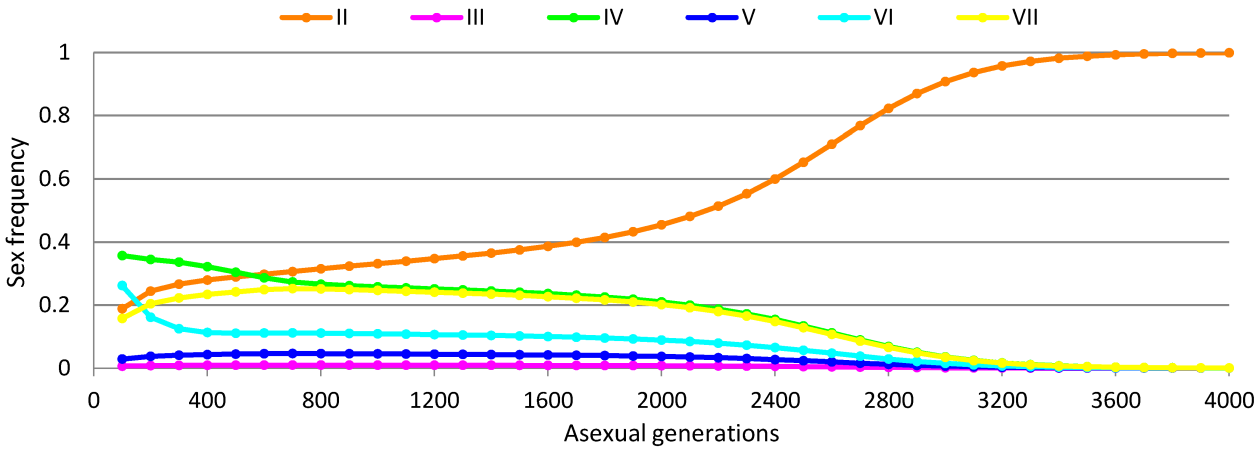
II
III
IV
V
VI
VII
1
0.8
0.6
0.4
0.2
0
Sex frequency
0
400
800
1200
1600
2000
2400
2800
3200
3600
4000
Asexual generations

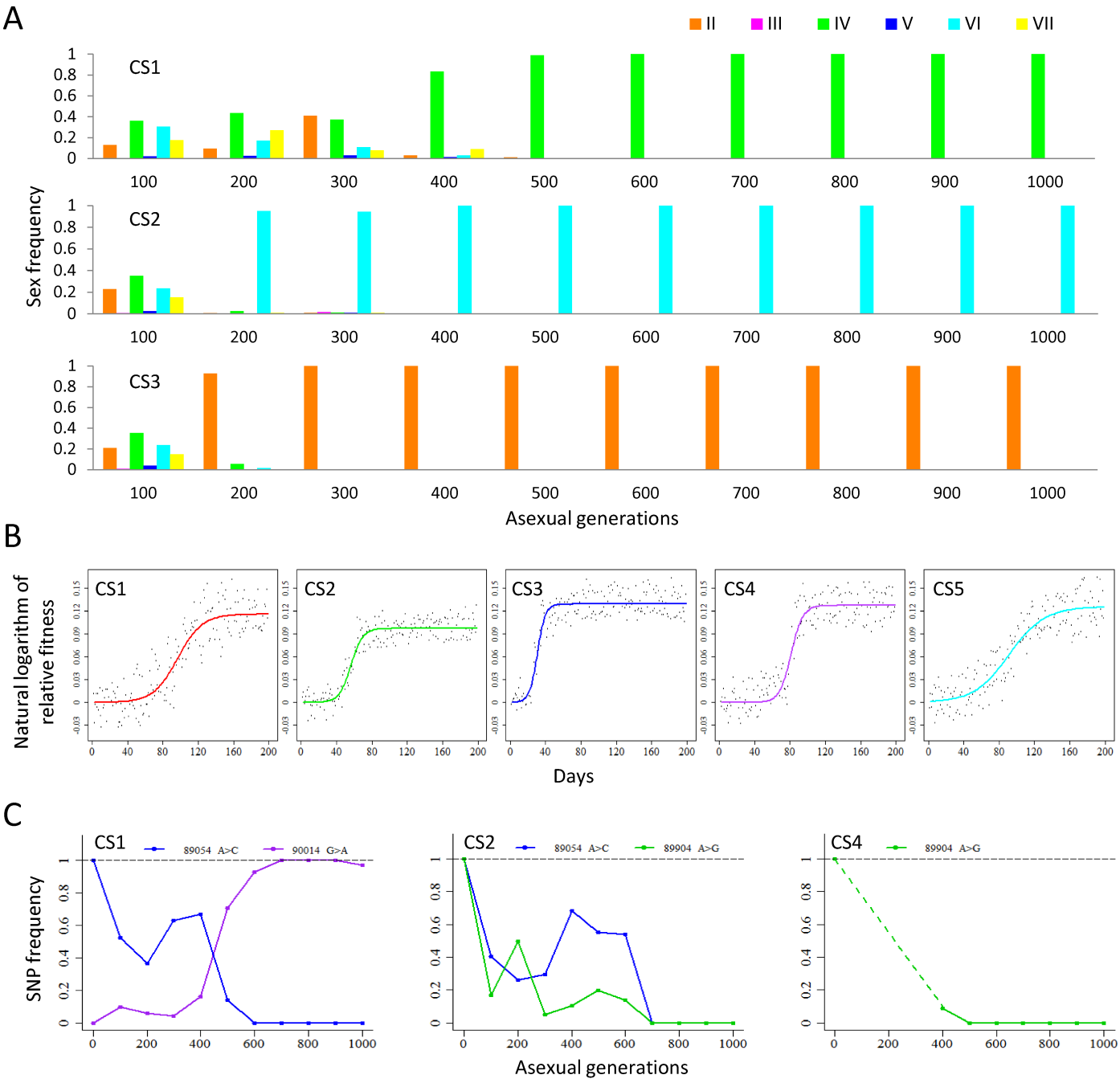
A
II
III
IV
V
VI
VII
CS1
CS2
CS3
Sex frequency
Asexual generations
B
CS1
CS2
CS3
CS4
CS5
Natural logarithm of relative fitness
Days
C
CS1
89054 A>C
90014 G>A
CS2
89054 A>C
89904 A>G
CS4
89904 A>G
SNP frequency
Asexual generations

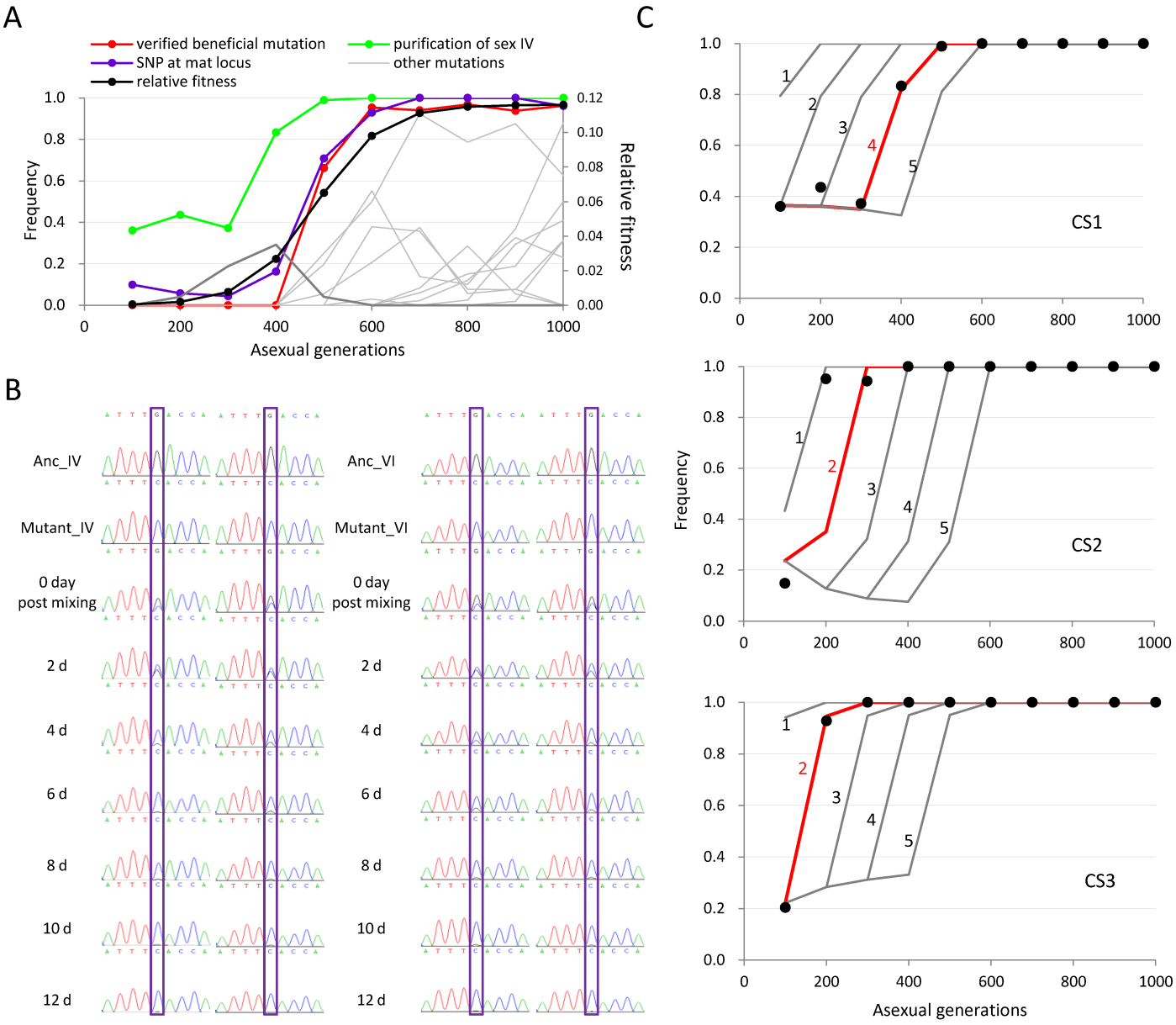
A
verified beneficial mutation
SNP at mat locus
relative fitness
purification of sex IV
other mutations
Frequency
Relative fitness
Asexual generations
B
Anc_IV
Mutant_IV
0 day post mixing
2 d
4 d
6 d
8 d
10 d
12 d
Anc_VI
Mutant_VI
C
CS1
CS2
CS3
Frequency
Asexual generations